ADVANCES IN APPLIED MATHEMATICS 16, 402–424 (1995)

Triangular Dissections, Aperiodic Tilings, and Jones Algebras

R. COQUEREAUX

Centre de Physique Théorique, CNRS Luminy-Case 907, F 13288 Marseille Cedex 9, France

The Brattelli diagram associated with a given bicolored Dynkin–Coxeter graph of type A_n determines planar fractal sets obtained by infinite dissections of a given triangle. All triangles appearing in the dissection process have angles that are multiples of $\pi/(n+1)$. There are usually several possible infinite dissections compatible with a given n but a given one makes use of $n/2$ triangle types if n is even. Jones algebra with index $[4\cos^2(\pi/(n+1))]^{-1}$ (values of the discrete range) act naturally on vector spaces associated with those fractal sets. Triangles of a given type are always congruent at each step of the dissection process. In the particular case $n = 4$, there are isometric and the whole structure lead, after proper inflation, to aperiodic Penrose tilings. The "tilings" associated with other values of the index are discussed and shown to be encoded by equivalence classes of infinite sequences (with appropriate constraints), using $n/2$ digits (if- n is even) and generalizing the Fibonacci numbers.

1. INTRODUCTION

The aim of this paper is to show how to associate infinite (fractal-like) dissections of triangles to Brattelli diagrams describing Jones algebras. We limit our discussion to those algebras related with the A_n series.

In Section 2, before describing the general features of the construction, we study in detail the case $n = 6$. As we shall see, there are essentially three different solutions of the dissection problem for this value of n. What we mean by a "solution" will become clear later. We then also discuss the relatively trivial cases $n = 3$ and $n = 4$. The choice $n = 4$ is actually not really trivial, since it is related to Penrose tilings, but the determination of the triangle types appearing in the dissection process is quite simple (only one solution). We finally give (without pictures) the six solutions corresponding to the case $n = 8$.

0196-8858/95 $12.00

In Section 3, we remind the reader what Jones algebras are and how to relate those associated with A_n Dynkin diagrams to the fractal sets built in the previous section.

In Section 4, following [2], we first explain why the Jones algebra associated with the Dynkin diagram of A_4 can be considered as a "non-commutative" description of the set of Penrose tilings. We then return to the case of A_n and introduce (finite or infinite) sequences that encode paths on Brattelli diagrams. We show finally how such sequences are in one to one correspondence with the triangles appearing in the dissection process described in the first part.

In Section 5, we make a few remarks relating our fractal dissection of triangles to the projection technique used, for instance, in the theory of quasicrystals.

2. Triangular Dissections Associated with A_n Diagrams

Let A_n be a Dynkin–Coxeter diagram, i.e., a sequence of n vertices linked by single edges. We shall actually consider bicolored graphs of the following type: odd and even vertices will be decorated with different colors. We now fold the diagram in such a way that odd vertices are on the first line and even vertices on the second line, as in Fig. 1 (example of A_6). We then attach the integer 1 to the vertices of the first line and label the second line with 1's or 2's by imposing downward propagation and conservation of the sum of integers ($2 = 1 + 1$), like in the usual Pascal's triangle.

To the previous bicolored simply connected graph (drawn on two lines), we now attach an infinite tower called the associated Brattelli diagram. Its construction is very elementary: We first reflect the previous two lines with respect to the horizontal and propagate the whole structure downward by the same procedure. The vertices are then labeled with integers by using downward propagation (as in Fig. 2), like in the Pascal's triangle.

It is convenient to parameterize lines of this diagram by an integer t. We assume that $t = 1$ corresponds to the first line of the diagram, $t = 2$ to the second line, etc. Note that the numbers labeling the vertices also correspond to the numbers of paths originating from the top line, propagating

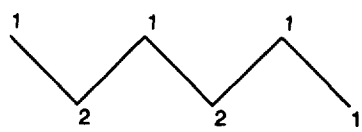

Fig. 1. The bicolored Coxeter–Dynkin graph of A_6.

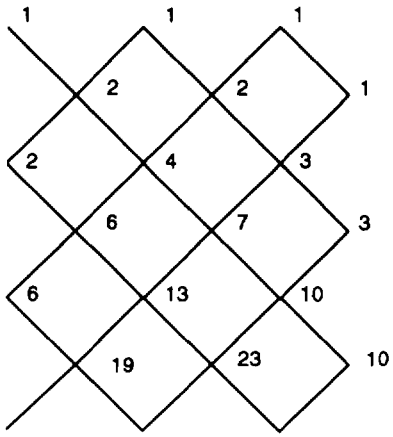

FIG. 2. The Brattelli diagram associated with the graph of A_6 (Jones algebra of index $4\cos^2 \pi/7$)

downward, and ending on the chosen vertex. For this reason, these numbers can also be considered as parameterizing random walks on a Dynkin diagram and t as a discrete time parameter.

It is clear that such a construction is not limited to Dynkin–Coxeter diagrams of type A_n but we shall not study more sophisticated examples in the present paper. The definitions of a Brattelli diagram has its origin in the theory of $\mathbb{C}^*$-algebras [1] and we shall actually need a few results from this theory in Section 3, but in the above elementary definition of a Brattelli diagram is sufficient for our purposes.

Rather than working with an arbitrary value of n we decide to explain this construction in the case $n = 6$. Cases n even and n odd are actually slightly different. We shall return to general values of n at the end of this section.

We take $n = 6$. Setting $l = n + 1 = 7$, we consider triangles with angles that are multiples of $\pi/7$. There is only a finite number of such triangles and they are obtained by decomposing 7 into a sum of three integers. Here are the possibilities:

$$
\begin{aligned}
7 &= 1 + 1 + 5 \qquad \alpha \doteq \langle 1,1,5 \rangle \\
7 &= 2 + 2 + 3 \qquad \beta \doteq \langle 2,2,3 \rangle \\
7 &= 3 + 3 + 1 \qquad \gamma \doteq \langle 3,3,1 \rangle \\
7 &= 4 + 2 + 1 \qquad \tilde{\pi} \doteq \langle 4,2,1 \rangle \\
7 &= 4 + 1 + 2 \qquad \pi \doteq \langle 4,1,2 \rangle .
\end{aligned}
$$

The first three triangles α, β, γ are isosceles and the last two π and $\tilde{\pi}$ are mirror images. We label the three angles in trigonometrical order, for example, $\pi = \langle 1,2,4\rangle = \langle 4,1,2\rangle = \langle 2,4,1\rangle \neq \tilde{\pi}$. These five triangles appear in the heptahedron (Fig. 3).

Each of these triangles can be decomposed into a union of two triangles belonging to the above family. A straightforward analysis leads to the following disintegration table

$$\begin{array}{llll}
\alpha \to \alpha + \pi, & \tilde{\pi} + \gamma, & \pi + \gamma, & \tilde{\pi} + \alpha \\
\beta \to \beta + \pi, & \pi + \gamma, & \tilde{\pi} + \gamma, & \tilde{\pi} + \beta \\
\gamma \to \pi + \gamma, & \tilde{\pi} + \gamma, & \beta + \alpha, & \alpha + \beta \\
\pi \to \alpha + \tilde{\pi}, & \alpha + \beta & \tilde{\pi} + \beta, & \tilde{\pi} + \gamma \\
\pi \to \alpha + \pi, & \alpha + \beta, & \pi + \beta, & \pi + \gamma.
\end{array}$$

We now want to interpret edges of the Brattelli diagrams as describing decomposition of triangles. The whole set of equations will be determined by the first three lines of this diagram. We first label the first two lines (i.e., the Coxeter–Dynkin diagram) with six unknown parameters $x\ y\ z\ t\ u\ v$, in this order, by following the diagram. We impose the following constraint: Triangle types appearing at step t of the dissection process should be the same as those appearing at step $t - 2$. It may be that more general rules could also give rise to interesting patterns but we shall impose this constraint in the present paper. This implies, in particular, that the third

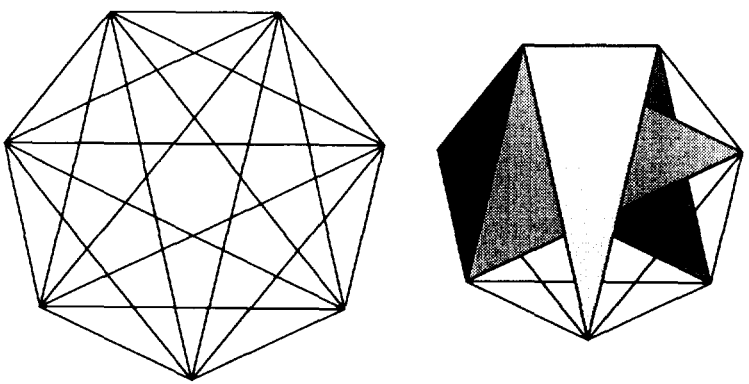

FIG. 3. A regular heptahedron displaying triangles of types $\alpha, \beta, \gamma, \pi, \tilde{\pi}$.

line has to be labeled as the first (with $x\,z\,u$); see Fig. 4. These parameters will ultimately be identified with particular triangles. The pattern of edges impose the constraints

$$x \to y$$
$$z \to y + t$$
$$u \to t + v$$
$$y \to x + z$$
$$t \to z + u$$
$$v \to u.$$

Therefore $x = y$ and $u = v$. We are left with four unknown parameters, $x\,z\,t\,u$, and four constraints,

$$z \to x + t$$
$$u \to t + u$$
$$x \to x + z$$
$$t \to z + u.$$

In order to solve these constraints, we have to make use of the disintegration table for triangles α, β, γ, π, and $\bar{\pi}$ given before. We also take into account the fact that the set of solutions is invariant by the transformation $x \leftrightarrow u, z \leftrightarrow t$ (the corresponding dissections are exactly the same). A rather tedious analysis (straightforward but cumbersome) leads to the following complete set of nine solutions. Here, we give the list the solutions by giving $x\,z\,t\,u$, in this order:

$$x = \langle 1,3,3\rangle,\ z = \langle 1,4,2\rangle,\ t = \langle 1,2,4\rangle,\ u = \langle 1,3,3\rangle$$
$$x = \langle 1,3,3\rangle,\ z = \langle 1,4,2\rangle,\ t = \langle 1,2,4\rangle,\ u = \langle 2,2,3\rangle$$
$$x = \langle 1,1,5\rangle,\ z = \langle 1,2,4\rangle,\ t = \langle 1,4,2\rangle,\ u = \langle 1,3,3\rangle$$
$$x = \langle 1,1,5\rangle,\ z = \langle 1,2,4\rangle,\ t = \langle 1,4,2\rangle,\ u = \langle 1,1,5\rangle$$
$$x = \langle 1,1,5\rangle,\ z = \langle 1,2,4\rangle,\ t = \langle 1,4,2\rangle,\ u = \langle 2,2,3\rangle$$
$$x = \langle 1,1,5\rangle,\ z = \langle 1,4,2\rangle,\ t = \langle 1,2,4\rangle,\ u = \langle 2,2,3\rangle$$
$$x = \langle 1,3,3\rangle,\ z = \langle 1,2,4\rangle,\ t = \langle 1,4,2\rangle,\ u = \langle 1,1,5\rangle$$
$$x = \langle 1,3,3\rangle,\ z = \langle 1,2,4\rangle,\ t = \langle 1,4,2\rangle,\ u = \langle 2,2,3\rangle$$
$$x = \langle 2,2,3\rangle,\ z = \langle 1,2,4\rangle,\ t = \langle 1,4,2\rangle,\ u = \langle 2,2,3\rangle.$$

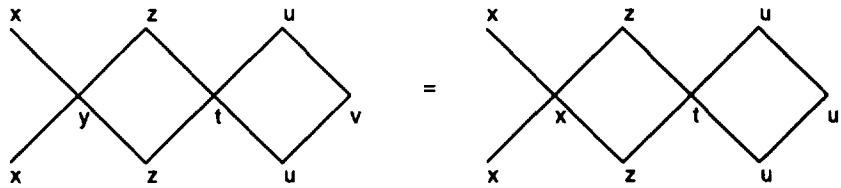

FIG. 4. The constraint equations for triangular dissections of type A_6.

We may impose the following extra condition: The three types of triangles that appear at a given line should be of three different types, i.e., $x \neq z$, $x \neq u$, and $z \neq u$. This arbitrary requirement can be relaxed if we can use color or gray levels in the pictures. Such a condition excludes, for example, the first solution,

$$x = \langle 1,3,3 \rangle = \gamma,\ z = \langle 1,4,2 \rangle = \tilde{\pi},$$
$$t = \langle 1,2,4 \rangle = \pi,\ u = \langle 1,3,3 \rangle = \gamma,$$

as well as the fourth and the last. Note that these excluded solutions minimize the set of "proto-triangles" (the elementary triangle types used in the construction). With the above condition, we are then left with six solutions, namely (we give here the full list of proto-triangles, $x\,x\,z\,t\,u\,u$),

$$\langle 1,3,3 \rangle,\ \langle 1,3,3 \rangle,\ \langle 1,4,2 \rangle,\ \langle 1,2,4 \rangle,\ \langle 2,2,3 \rangle,\ \langle 2,2,3 \rangle$$
$$\langle 1,1,5 \rangle,\ \langle 1,1,5 \rangle,\ \langle 1,2,4 \rangle,\ \langle 1,4,2 \rangle,\ \langle 1,3,3 \rangle,\ \langle 1,3,3 \rangle$$
$$\langle 1,1,5 \rangle,\ \langle 1,1,5 \rangle,\ \langle 1,2,4 \rangle,\ \langle 1,4,2 \rangle,\ \langle 2,2,3 \rangle,\ \langle 2,2,3 \rangle$$
$$\langle 1,1,5 \rangle,\ \langle 1,1,5 \rangle,\ \langle 1,4,2 \rangle,\ \langle 1,2,4 \rangle,\ \langle 2,2,3 \rangle,\ \langle 2,2,3 \rangle$$
$$\langle 1,3,3 \rangle,\ \langle 1,3,3 \rangle,\ \langle 1,2,4 \rangle,\ \langle 1,4,2 \rangle,\ \langle 1,1,5 \rangle,\ \langle 1,1,5 \rangle$$
$$\langle 1,3,3 \rangle,\ \langle 1,3,3 \rangle,\ \langle 1,2,4 \rangle,\ \langle 1,4,2 \rangle,\ \langle 2,2,3 \rangle,\ \langle 2,2,3 \rangle.$$

It is easy to see that the set of solutions is invariant by the transformation $\pi \leftrightarrow \tilde{\pi}$. We are finally left with the three solutions,

$$\alpha\ \alpha\ \pi\ \tilde{\pi}\ \beta\ \beta$$
$$\gamma\ \gamma\ \pi\ \tilde{\pi}\ \alpha\ \alpha$$
$$\gamma\ \gamma\ \pi\ \tilde{\pi}\ \beta\ \beta.$$

The other three solutions are obtained from the previous ones by taking their mirror images. In this example of A_6 there is no further ambiguity in

the dissection process; in particular, the choice of one of the two equal angles of isosceles triangles determining a particular cutting is fixed by the requirement that, depending upon the case, and as specified by the above table of solutions, either π or $\tilde{\pi}$ should appear as an offspring. This is not a generic feature valid for all values of n (it is even wrong when $n = 4$, as we shall see below).

The solution $\alpha\alpha\pi\tilde{\pi}\beta\beta$ is illustrated in Fig. 5 (steps $t = 1, t = 2, t = 3$, $t = 3, t = 9, t = 10$).

The solutions $\gamma\gamma\pi\tilde{\pi}\alpha\alpha$ and $\gamma\gamma\pi\tilde{\pi}\beta\beta$ give rise to analogous pictures.

Figure 16 shows in particular how 352 triangles of type α, 197 triangles of type β, and 441 triangles of type $\tilde{\pi}$ fit together to build a partition (line $t = 11$ of the Brattelli diagram of Fig. 2) of their common ancestor, a "big" triangle that is itself a union of one α, one β, and one π and corresponds to line 1 of the same Brattelli diagram. All these pictures were generated by a computer program written using MATHEMATICA.

Note that no solution involves all five triangles α, β, γ, π, and $\tilde{\pi}$ simultaneously.

We discussed above the case associated with the Dynkin diagram of A_n with $n = 6$. For other values of n, one proceeds exactly in the same way. First, one establishes the list of possible triangles (with angles that are integer multiple of $\pi/(n + 1)$) by looking at partitions of $n + 1$. Then, by solving the equations for constraints, associated with the corresponding Brattelli diagram, one chooses a solution and, accordingly, selects n types of triangles. Actually, when $n = 2m$ is even, because the $\mathbb{Z}_2$ symmetry of the Coxeter–Dynkin diagram, one needs only m types of triangles, along with their mirror image—this makes no difference when the triangle is isosceles! Therefore m types will appear at even times $2t$ and their mirror images will appear at odd times $2t + 1$. Since all solutions to constraint equations appear along with their mirror images, one can shorten the total list of solutions for constraints (it is enough to give a reduced list).

Note that discussion of the case $n = 3$ is very simple. The corresponding Coxeter–Dynkin graph and associated Brattelli diagrams are shown in Fig. 6. The associated dissections involve only isosceles triangles with angles $\langle \pi/4, \pi/4, \pi/2 \rangle$ since $l = n + 1 = 4 = 1 + 1 + 2$. At time t, the ancestor traingle contains 2^t small triangles (if t is even) and $2^t + 2^t$ if t is odd. The alert reader recognizes the dimensions of the complexified Clifford algebras. We shall return to that in the next section. Locally the dissected ancestor triangle looks like part of a square tiling of the plane (see Fig. 7).

The case A_4 is related with Penrose aperiodic tiling of the plane. Corresponding Coxeter–Dynkin graph and associated Brattelli diagrams are shown in Fig. 8. The possible triangles involved are obtained by writing $l = n + 1 = 5 = 3 + 1 + 1 = 1 + 2 + 2$. We set $\alpha = \langle 2, 2, 1 \rangle$ and $\beta = \langle 1, 1, 3 \rangle$. Elementary disintegrations are $\alpha \to \alpha + \beta$ and $\beta \to \alpha + \beta$. The

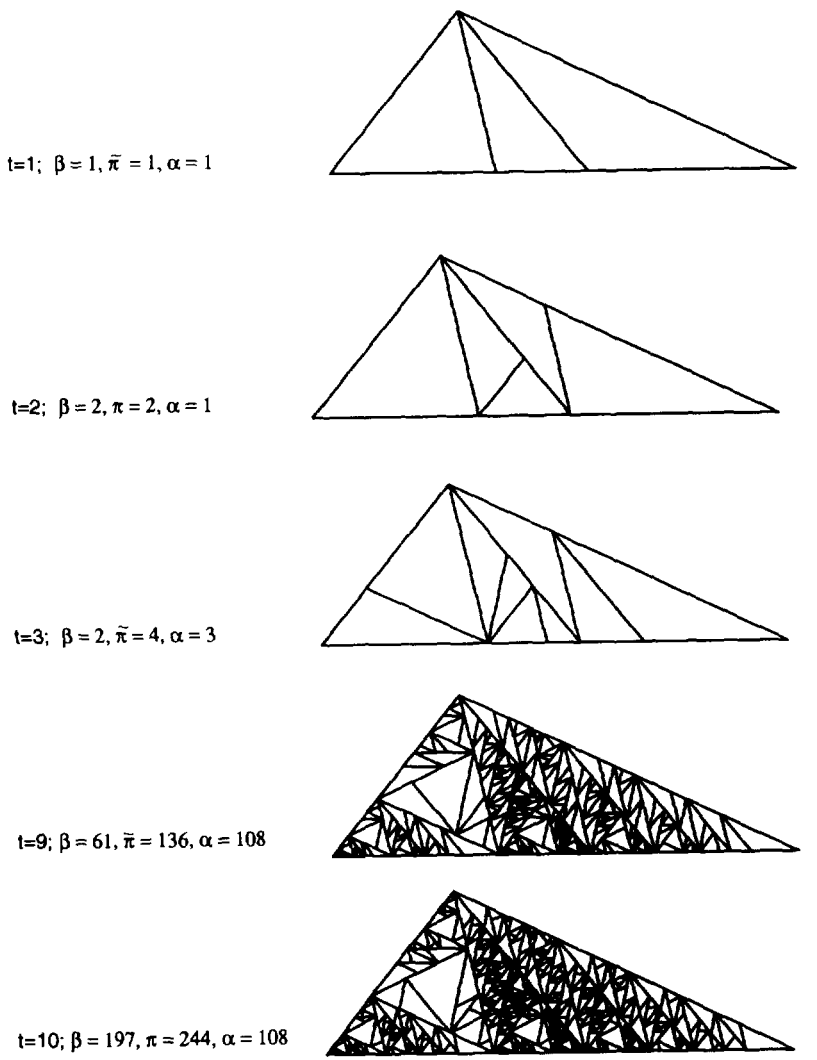

FIG. 5. Dissection of a triangle $\langle 4, 2, 1\rangle$ $\pi/7$ according to the embeddings specified by the Brattelli diagram associated with a bicolored Coxeter-Dynkin graph of A_6.

constraints displayed in Fig. 9 lead to the following equations:

$$x \to x + y$$
$$y \to x + y.$$

The solution is obviously $x = \alpha$ and $y = \beta$, or the converse. The dissection of the ancestor triangle (of type α, for example) is, however, not

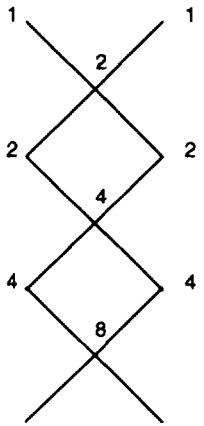

FIG. 6. The Brattelli diagram associated with the Coxeter–Dynkin graph of A_3 (Jones algebra of index $4\cos^2 \pi/4 = 2$, i.e., Clifford algebra).

entirely determined by the previous rule. Indeed, there are two possible ways of cutting triangle α (and two others for triangle β). More generally, once the triangles are oriented, one could change the cutting rule at each step. In other words, a solution to the set of constraints specified by a given Brattelli diagram does not always specify the cutting rules (there was no ambiguity for the solutions associated with the A_6 diagram but there are different choices for A_4). Two such possible choices are illustrated now: One can cut the first or the second angle (both equal to $2\pi/5$) of $\langle 2, 2, 1\rangle$. These two possibilities read (we label vertices by capital letters $\alpha = ABC$, $\beta = DEF$, along with associated angles as a subscript, in units of $\pi/5$; M and N are the new vertices appearing in the dissection of α and

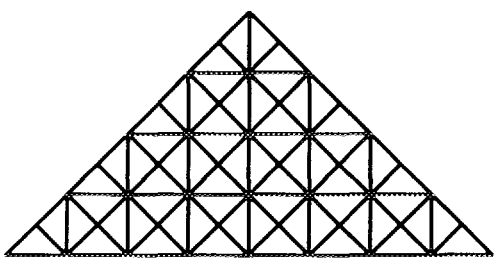

FIG. 7. Case of A_3. Dissection of a triangle $\langle 1, 1, 2\rangle$ $\pi/4$ into a union of 64 triangles. Step $t = 6$.

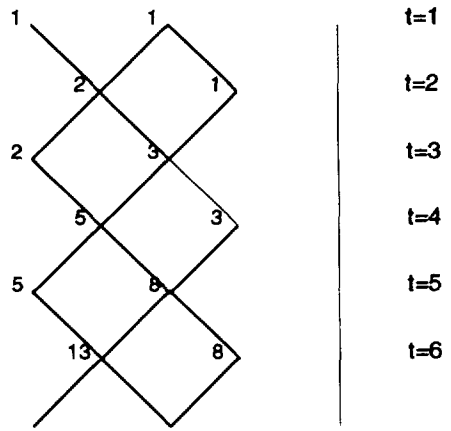

FIG. 8. The Brattelli diagram associated with the Coxeter–Dynkin graph of A_4 (Jones algebra of index $4\cos^2 \pi/5 = 1/\phi^2$).

β)

$$\langle A_1 B_2 C_2 \rangle \to \langle C_1 M_1 B_1 \rangle + \langle C_1 M_3 A_1 \rangle$$

$$\langle D_3 E_1 F_1 \rangle \to \langle D_1 E_1 N_3 \rangle + \langle D_2 N_2 F_1 \rangle$$

or

$$\langle A_1 B_2 C_2 \rangle \to \langle A_1 B_1 M_3 \rangle + \langle B_1 C_2 M_2 \rangle$$

$$\langle D_3 E_1 F_1 \rangle \to \langle D_1 E_1 N_3 \rangle + \langle D_2 N_2 F_1 \rangle.$$

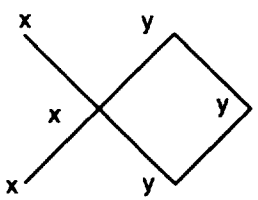

FIG. 9. The constraint equations for triangular dissections of type A_4.

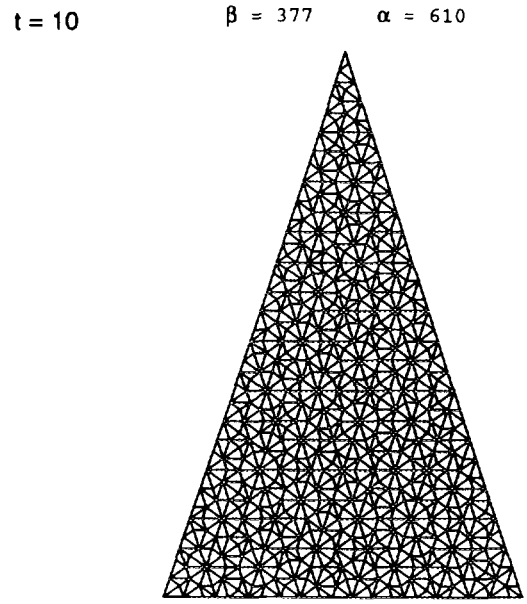

FIG. 10. Case of A_4. Penrose-like structure obtained by dissection of a triangle $\langle 2, 2, 1\rangle$ $\pi/5$. There are 610 + 377 triangles (Fibonacci numbers) belonging to two different families. Step $t = 14$.

Whatever dissection we choose as a starting point, propagating this choice downward to all levels of the infinite Brattelli tower, will lead at level $2t + 1$ to two kinds of triangles, F_{2t+1} of type α and F_{2t+2} of type β, where F_n are Fibonacci numbers ($F_n = F_{n-1} + F_{n-2}, F_0 = 0, F_1 = 1$). Choosing an ancestor triangle of type α, two such infinite dissections are illustrated at level $t = 13$ in Fig. 10 and Fig. 11 ($F_6 = 377$ triangles of type α and $F_7 = 610$ triangles of type β). Locally, the fractal triangular dissection of type A_4 illustrated in Fig. 10 looks like part of a Penrose tiling of the plane (the one illustrated in Fig. 11 does not).

In the case of Fig.10, calling $s_k = \sin(k\pi/5), c_k = \cos(k\pi/5), \phi = 4\cos^2(\pi/5) - 1 = 2\cos(\pi/5) = (1 + \sqrt{5})/2 = 1.618\ldots$ (the golden number), and $\hat{\phi} = -1/\phi = 1 - \phi$, we note that, if we normalize the area of the ancestor triangle (of type α) to 1, then, at level p (take it odd), al F_p triangles of type α have the same area, namely $(s_1/s_2)^{p+1}$, and all F_{p+1} triangles of type β have also the same area, namely $(s_1/s_2)^{p-2}c_2/c_1$. We can check unitarity for all values of t by writing Σ Area(α) + ΣArea(β) = 1. When $t \to \infty$, we see that Σ Area(α) $= -\hat{\phi}/\sqrt{5} = \phi - 1/\sqrt{5}$ and Σ Area(β) $= 1 + \hat{\phi}/\sqrt{5}$ (so that, of course, the total area is one).

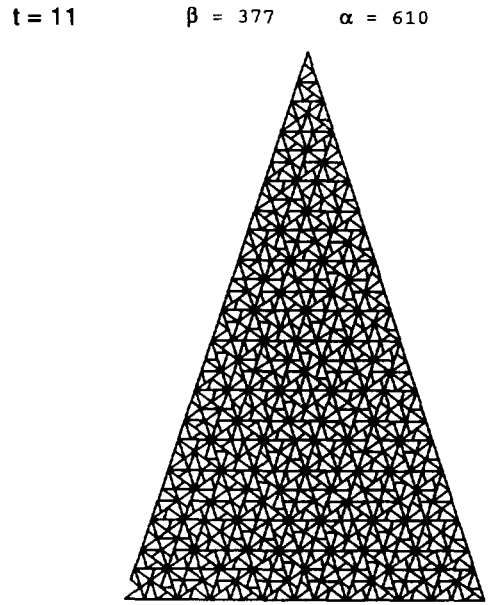

FIG. 11. Same as Fig. 10 but with a different choice for the elementary matching conditions.

The fact that all triangles of a given type have the same area at a given step of the dissection is a property of the case $n = 4$ but is not a generic feature of the construction. In the example, $n = 6$, for example, we saw that such triangles are congruent (similar) but not isometric in the Euclidean plane (see, for instance, Fig. 5). This property (the fact that one can make a partition of all triangles appearing at a given step into a finite number of types, all triangles belonging to a given type being congruent) is of course true, by construction, for all values of n. At this point, it may be useful to remember that $2\cos \pi/5$ is solution of a quadratic equation ($x^2 - x - 1 = 0$), whereas $2\cos \pi/7$ is solution of cubic equation ($x^3 - x^2 - 2x + 1 = 0$).

Triangle dissections for bigger values of n can be handled in a similar way. However, the combinatorics becomes quite involved. For instance, discussion of the case $n = 8$ involves 10 different types of triangles (with angles that are multiples of $\pi/9$) and the resolution by hand of the set of constraints is quite painful. The following table gives the set of solutions obtained thanks to a PROLOG-III computer program (we list the solutions ($a1 = a2, a3, a4, a5, a6, a7 = a8$) by following the connected vertices of the Coxeter–Dynkin diagram and only give solutions involving no

repetitions of triangle types, i.e., $a1 \neq a3, a1 \neq a5, a1 \neq a7, a1 \neq a4, a1 \neq a6, a3 \neq a5, a3 \neq a7, a4 \neq a6, a4 \neq a7, a6 \neq a7$):

$\langle 1,1,7\rangle$, $\langle 1,1,7\rangle$, $\langle 1,6,2\rangle$, $\langle 1,2,6\rangle$, $\langle 2,4,3\rangle$, $\langle 2,3,4\rangle$, $\langle 2,2,5\rangle$, $\langle 2,2,5\rangle$
$\langle 1,1,7\rangle$, $\langle 1,1,7\rangle$, $\langle 1,6,2\rangle$, $\langle 1,2,6\rangle$, $\langle 1,3,5\rangle$, $\langle 1,5,3\rangle$, $\langle 1,4,4\rangle$, $\langle 1,4,4\rangle$
$\langle 2,2,5\rangle$, $\langle 2,2,5\rangle$, $\langle 2,3,4\rangle$, $\langle 2,4,3\rangle$, $\langle 1,3,5\rangle$, $\langle 1,5,3\rangle$, $\langle 1,4,4\rangle$, $\langle 1,4,4\rangle$
$\langle 1,1,7\rangle$, $\langle 1,1,7\rangle$, $\langle 1,2,6\rangle$, $\langle 1,6,2\rangle$, $\langle 2,3,4\rangle$, $\langle 2,4,3\rangle$, $\langle 2,2,5\rangle$, $\langle 2,2,5\rangle$
$\langle 1,1,7\rangle$, $\langle 1,1,7\rangle$, $\langle 1,2,6\rangle$, $\langle 1,6,2\rangle$, $\langle 1,5,3\rangle$, $\langle 1,3,5\rangle$, $\langle 1,4,4\rangle$, $\langle 1,4,4\rangle$
$\langle 2,2,5\rangle$, $\langle 2,2,5\rangle$, $\langle 2,4,3\rangle$, $\langle 2,3,4\rangle$, $\langle 1,5,3\rangle$, $\langle 1,3,5\rangle$, $\langle 1,4,4\rangle$, $\langle 1,4,4\rangle$.

Other cases of A_n can be studied in the same way. One can in particular look at the interesting cases $n = 11$, $n = 17$, and $n = 29$ because of their relations with exceptional groups E_6, E_7, and E_8 (they have same Coxeter numbers, namely 12, 18, and 30).

3. Jones Algebras and Triangular Dissections

Jones algebras appeared as an important tool in the study of subfactors of Von Neumann algebras. It will be enough, for us, to give the following definition. τ being a real number, we call $\mathcal{A}(\tau)$ the involutive algebra defined by an infinite number of self-adjoint generators $\{e_1, e_2, \ldots, e_p, \ldots\}$ with relations

$$\begin{aligned} e_p \cdot e_p &= e_p \\ e_p \cdot e_{p\pm 1} \cdot e_p &= \tau e_p \\ e_p \cdot e_q &= e_q \cdot e_p \qquad \text{if } |q-p| \geq 2. \end{aligned}$$

Note that the e_p's are projectors. The condition of being self-adjoint is actually quite strong; it implies that $1/\tau$ cannot be arbitrary but must belong to the following set [8]:

$$\frac{1}{\tau} \in \{4\cos^2 \pi/(n+1)_{n\in\{2,3,4,\ldots\}}\} \cup [4, \infty[.$$

The quantity $Q \doteq 1/\tau$ is called the index. If one relax this condition of being self-adjoint, one obtains algebras for all values of τ. These algebras were introduced by Temperley and Lieb [19]; we shall call them Jones algebras since the $*$-condition is, for us, essential. Our triangular dissections are actually related to Jones algebras with index $1/\tau$ in the discrete range $\tau \in \{[4\cos^2 \pi/(n+1)]^{-1}\}_{n\in\{2,3,4,\ldots\}}$. Readers knowing Clifford algebras will have recognized that, in the case $\tau = \frac{1}{2}$, one can set $e_p = \frac{1}{2}(1 +$

$\gamma_p\gamma_{p+1}$), where the γ's generate the usual (infinite dimensional) Clifford algebra: $\gamma_p^2 = 1$, $\gamma_p\gamma_q + \gamma_q\gamma_p = 0$ if $p \neq q$. The algebra generated by the e_p then coincides, when $\tau = \frac{1}{2}$ with the even part of the infinite dimensional Clifford algebra. Looking at the infinite Brattelli diagram of A_3 displayed in Fig. 6 (one recognizes the dimensions of finite dimensional Clifford algebras) suggests then an alternative definition of Jones algebras (for general τ) which is totally explicit and actually better suited for our purposes.

We therefore consider the (infinite) Brattelli diagram as describing an infinite tower of matrix algebras, with embeddings specified by the edges on the diagram (this is actually why such diagrams were introduced in the first place [1]). For example, in the case of A_4, i.e., $\tau = 4\cos^2 \pi/5^{-1} = \phi^2$ (ϕ is the golden number), the lines $t = 3, t = 4$ read as Fig. 12. The first line describes a direct sum of two matrix algebras $M_2(\mathbb{C}) \oplus M_3(\mathbb{C})$ embedded in the matrix algebra $M_5(\mathbb{C}) \oplus M_3(\mathbb{C})$ as Fig. 13. The embedding was here quite easy to describe since A_n diagrams involve only single lines but this can be generalized. For a given value of the discrete time flow t (i.e., at the line t), we have an algebra $\mathscr{A}_t(\tau)$ that is a direct sum of finite dimensional algebras with dimensions specified by the integers appearing at level t. The Jones algebra is actually defined as the inductive limit of this sequence of algebras. We refer to 8, 9, 6, 4 for more information, but we can summarize the situation as follows. An essential ingredient of the construction is the existence of a trace Tr. The first remark is that, on a simple finite dimensional matrix algebra, the trace is unique, up to scale. This is not so on a direct sum of simple finite dimensional matrix algebras since any linear combination of component traces is a trace (in the sense that $\mathrm{tr}(a.b) = \mathrm{tr}(b.a)$). In the case of an infinite family such as the one defined by the Brattelli diagram of A_4, it is possible to define a trace at each line t of the diagram, in such a way that it is compatible with the embedding defined by the diagram. This property allows one to define a *unique* trace Tr on all the algebras $\mathscr{A}_t(\tau)$. For example, in the case $n = 4$, i.e., $\tau = \phi^2$, the trace Tr can be explicitly defined at level $2t + 1$, where $\mathscr{A}_t(\tau) = M_{F_{2t+1}}(\mathbb{C}) \oplus M_{F_{2t+2}}(\mathbb{C})$ by

$$\mathrm{Tr} = \tau^{t+1}\,\mathrm{tr}_\alpha + \tau^t(1-\tau)\mathrm{tr}_\beta$$

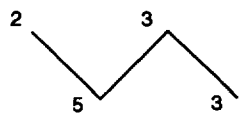

FIG. 12. Part of the Brattelli diagram associated with a bicolored Dynkin–Coxeter graph of type A_4.

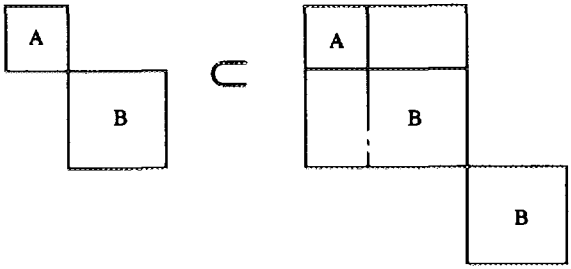

FIG. 13. Embedding of algebras described by the diagram of Fig.12.

and at level $2t$, where $\mathscr{A}_t(\tau) = M_{F_{2t-1}}(\mathbb{C}) \oplus (M_{F_{2t}}(\mathbb{C})$ by

$$\mathrm{Tr} = \tau^t \,\mathrm{tr}_\alpha + \tau^{t-1}(1-\tau)\mathrm{tr}_\beta,$$

where tr_α and tr_β denote the "naive" traces on the corresponding simple factors. The reader can verify that such a definition is indeed compatible with the specified embeddings. It can then be checked that

$$\mathrm{Tr}(xe_{n+1}) = \tau\,\mathrm{Tr}(x)$$

if x belongs to the algebra generated by $1, e_1, e_2, \ldots, e_n$. In particular, $\mathrm{Tr}(e_n) = \tau$. This trace Tr is also used to give a topology of $\mathbb{C}^*$ algebra to the inductive limit. This is the Jones algebra $\mathscr{A}(\tau)$. Its weak closure is a Von Neumann factor of type II_1 (there is a trace!)

The trace of projectors obviously belongs to the set $\mathbb{Z} \oplus \mathbb{Z}$ (in the case $n = 4$) or to the set $\mathbb{Z} \oplus \ldots \oplus \mathbb{Z}$ ($2m$ times) in the case of A_{2m}. This discussion leads to the study of the K-theory of algebras $\mathscr{A}(\tau)$ and we refer to [2, 3] for a discussion of the case $\tau = \phi^2$, where it is shown that $K_0(\mathscr{A}(\tau)) = \mathbb{Z} \oplus \tau\mathbb{Z}$. Note that the first two lines of diagram (Fig. 12) describing the inclusions and determining the infinite Brattelli diagram are fully specified by the positive matrix

$$\begin{pmatrix} 1 & 1 \\ 1 & 0 \end{pmatrix}$$

and that the largest eigenvalue of this matrix is precisely equal to τ. For more information about Brattelli diagrams, graphs, incidence matrices, and Perron–Frobenius vectors, we refer to [6].

We shall return a little bit later to Jones algebras but note already that they are naturally represented on the fractal sets described in the previous section. By this, we mean the following: Take for example $n = 6$ (i.e., $\tau = 1/(4\cos^2(\pi/7))$ and $t = 4$; we can decorate all $6 + 7 + 3 = 16$ trian-

gles appearing at that level with particular complex numbers (or colors) and put this information in a column vector with 16 components. The matrix algebra $\mathscr{A}_{t=4}(\tau) = M_6(\mathbb{C}) \oplus M_7(\mathbb{C}) \oplus M_3(\mathbb{C})$ acts on the vector space $\mathbb{C}^{16} = \mathbb{C}^6 \oplus \mathbb{C}^7 \oplus \mathbb{C}^3$ spanned by such vectors. In other words, the set of all triangles appearing at level t provides a basis for a representation of the algebra $\mathscr{A}_t$. The different sets of triangles associated with a given type (there are three of them in this example) correspond to the irreducible representations of the semi-simple algebra $\mathscr{A}_t(\tau)$.

4. Infinite Sequences, Non-commutative Geometry and Aperiodic Tilings

We start with the discussion of A_4. Note first that a tiling by Penrose kites and darts gives rise to a tiling using the two kinds of triangles discussed in the first section if we simply cut the kite and the dart into two equal triangular pieces.

It is known (for example, [7]) that there exists an infinite number (cardinality of the continuum) of inequivalent (aperiodic) Penrose tilings of the plane. It is also known (see the nice discussion in [5]) that each finite part of a given tiling can be found (an infinite number of times) in any other tiling. Each Penrose tiling can be encoded by an infinite sequence of 0 and 1, obeying the following rule: 1 is isolated. Such a sequence gives actually a construction procedure for a Penrose tiling (sometimes called a "Penrose universe"). Two sequences that differ only by a finite number of terms define the same tiling (only the chosen "origin" is different). Two such sequences are declared equivalent when they differ by a finite number of terms (i.e., they agree after some rank t). The space of equivalence classes is then a Cantor set (measure 0 and cardinality of $\aleph_1 = 2^{\aleph_0}$). The above are standard results. We shall reinterpret them below.

Non-commutative geometry, as described in [3] gives us a new way of encoding equivalence classes (or more generally groupoids); this description uses (non-commutative) algebras rather than (quotient) sets. In the case of finite dimensions, rather than collapsing an equivalence class (with p elements) to a single point, one describes it by a full matrix algebra $M_p(\mathbb{C})$. In the present case of Penrose tilings, one [3] declares that two finite sequences of 0 and 1 (satisfying the rule "1 is isolated") are equivalent if they end by the same digit. It is easy to check that there are F_t such sequences of length t ending by 0 and F_{t-1} such sequences of length t ending by 1. For each value of t we have therefore two equivalence classes; according to the philosophy of non-commutative geometry, they are encoded by the algebra $M_{F_t} \oplus M_{F_{t-1}}$, i.e., by $\mathscr{A}_t(\tau)$, with $\tau = \phi^2$.

There is a projection from the space of sequences of length t to the space of sequences of length $t-1$; it is obtained by erasing the last digit. One can see that, correspondingly, there is an inclusion from the algebra $\mathcal{A}_{t-1}(\tau)$ into the algebra $\mathcal{A}_t(\tau)$. This inclusion coincides with the one described by the Brattelli diagram. One can (and must), of course, consider infinite sequences; Penrose tilings are described by equivalence classes of infinite sequences. Corresponding to the projective limit of sequences we have an inductive limit of algebras. In other words, non-commutative geometry encodes the space of inequivalent Penrose tilings by the Jones algebra $\mathcal{A}(\phi^2)$. This is, in essence the message of Chap. II-3 of the book [3]; see also [2].

An infinite sequence of the previous kind also describes a never ending path on the Brattelli diagram, i.e.,. an infinite dive within the fractal set obtained by infinite dissection in the first part of this article. The correspondence between sequences of triangles and sequences of 0 and 1 will be discussed shortly. Using triangular dissection to generate Penrose tilings is a known technique (it was advocated, for example, in the book [20]). What is important to note here is that the fractal triangle of type A_4 constructed in Section 2 contains, in a sense, *all* Penrose tilings; it is, in a sense, analogous to the Mandelbrot set that encodes all possible Julia sets. Indeed, an infinite dive in this fractal triangle describes a particular Penrose tiling. A finite dive (at depth t) corresponds to the choice of a specific triangle appearing at a finite value of t. If we inflate this triangle by the proper scale (some power of the golden number), it can be super-imposed onto the first "ancestor-triangle" and we obtain in this way an aperiodic tiling of part of the plane. Equivalently, we can "cut a window" around the chosen small triangle and inflate it. The fact that following a path along the Brattelli diagram (or choosing triangles within triangles) ultimately defines a tiling of the plane is ensured by the hierarchical nature of the construction and, in particular, by the compatible embeddings of all algebras $\mathcal{A}_t(\tau)$, i.e., by the definition and existence of $\mathcal{A}(\tau)$ as an inductive limit.

Now, there is nothing special about $n = 4$. Other "fractal triangles" corresponding to Coxeter–Dynkin graphs of type A_n have been constructed in the first section and they play the same role as above. As in the case of A_4 it may be useful to define directly new kinds of infinite sequences with appropriate constraints along with an equivalence relation, in such a way that the Jones algebra $\mathcal{A}(\tau)$ appears *a priori* as the non-commutative object encoding the space of equivalence classes. Let us give the construction rules for such sequences in a few cases. The simplest of all is certainly the case A_3 that is encoded by the Clifford algebras ($\tau = \frac{1}{2}$). The associated finite sequences of length t are just sequences of 0 and 1 with no particular constraint. Two finite sequences are equivalent if

they end with the same digit and there are clearly 2^{t-1} such equivalent sequences at level t.

For a general bicolored Dynkin–Coxeter graph, the following technique obviously works (but as we shall see it can be improved in the case of A_{2m}): We label red (say) vertices by integers $1, 2, 3\ldots$ and green (say) vertices by letters $\alpha, \beta, \gamma\ldots$. We build sequences starting by $1, 2, 3\ldots$ containing both integers and Greek letters with the following constraint; a symbol x can be followed by the symbol y if x and y are linked on the Dynkin–Coxeter graph. The numbers of equivalent finite sequences (i.e., sequences ending by the same symbol) of given length are given by the integers appearing on the associated Brattelli diagram. For example, in the case of A_4 and for $t = 4$, we obtain the following words $1\alpha 1\alpha$, $1\alpha 2\alpha$, $2\alpha 1\alpha$, $2\alpha 2\alpha$, $2\beta 2\alpha$ and $1\alpha 2\beta$, $2\alpha 2\beta$, $2\beta 2\beta$, i.e., three sequences ending with β and five sequences ending with α (Fibonacci numbers, of course). But we already know that, in the case of A_4 it is enough to consider sequences containing only two symbols (0 and 1) that obey the rule: 1 is isolated. More generally and thanks to $\mathbb{Z}_2$ symmetry, the rules for A_n can be simplified when n is even ($n = 2m$). In that case, we fold the Dynkin–Coxeter graph "over itself" and obtain a string of $m = n/2$ vertices, the first one being related to itself by a closed loop (see Fig. 14 for the case of A_6). We then label the vertices from 0 to $m - 1$ and decide to build sequences that start by integers taken from the set $0, 1, \ldots, m - 1$ and that obey the following constraint: the symbol x can be followed by the symbol y if they are linked (neighbors) in the list $0 \leftrightarrow 0 \leftrightarrow 1 \leftrightarrow 2 \leftrightarrow \ldots \leftrightarrow m - 1$. For instance, the constraints for A_6 read $0 \leftrightarrow 0 \leftrightarrow 1 \leftrightarrow 2$. It is a simple combinatoric exercise to check that the number of finite sequences of length t obeying the previous rules and ending by the same given digit is again given by the integers appearing at depth t on the associated Brattelli diagram. Such sequences of length t encode paths of the Brattelli diagram starting at the top level $t = 1$ and ending at depth t. The correspondence goes as follows: We again draw the Brattelli diagram but this time, we label vertices from left to right with integers $2, 0, 1$ when t is odd but with integers $1, 0, 2$ again from left to right, when t is even (see Fig. 15 in the case of A_6). A sequence of the previous kind clearly labels a path from top to bottom by following the corresponding integers (the path

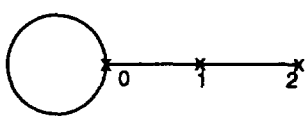

FIG. 14. Diagram obtained by folding the graph of A_6 over itself. It describes sequences obeying the rule $0 \leftrightarrow 0 \leftrightarrow 1 \leftrightarrow 2$.

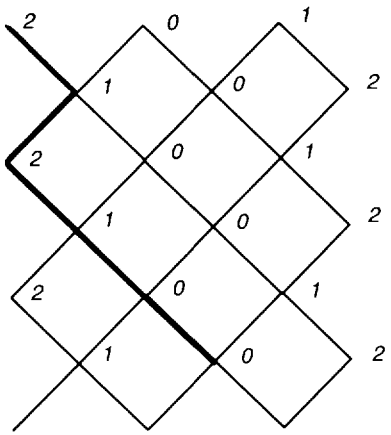

FIG. 15. A path on the Brattelli diagram of A_6 characterized by the sequence $2-1-2-1-0-0$.

2, 1, 2, 1, 0, 0 is highlighted on Fig. 15). This sequence, in turn, specifies a particular triangle of the dissection process. We have seen that the Jones algebra associated with some value of τ acts on a vector space for which we can choose a basis labeled by the space X of triangles of the dissection process. We can, of course, replace these triangles by paths or by sequences. What is nice with triangles is that one can "see" them! Before ending this sub-section devoted to sequences encoding paths and their relations with triangular dissections, let us remember that Fibonacci numbers (i.e., case of A_4) define the Fibonacci number system [14]. We can represent any nonnegative integer n as a sequence of 0's and 1's writing

$$n = (b_m b_{m-1} \cdots b_2) \Leftrightarrow n = \sum_{k=2}^{m} b_k F_k .$$

This system is like binary notation, except that there are never two adjacent 1's. For instance, $7 = 5 + 2 = F_4 + F_2 = (1010)$. Incidentally this property allows one to give a particular total ordering to the space of finite paths of the Brattelli tower of A_4, or equivalently, to the space of triangles appearing after a finite number of dissections. The other sequences of type A_k (dimension of finite dimensional Jones algebras) for all k appear like generalizations of the Fibonacci number system. Note that it is possible to give an algebra structure to the set of discrete strings (paths) living on the kind of diagrams that we discuss in the present paper [17]; this algebra

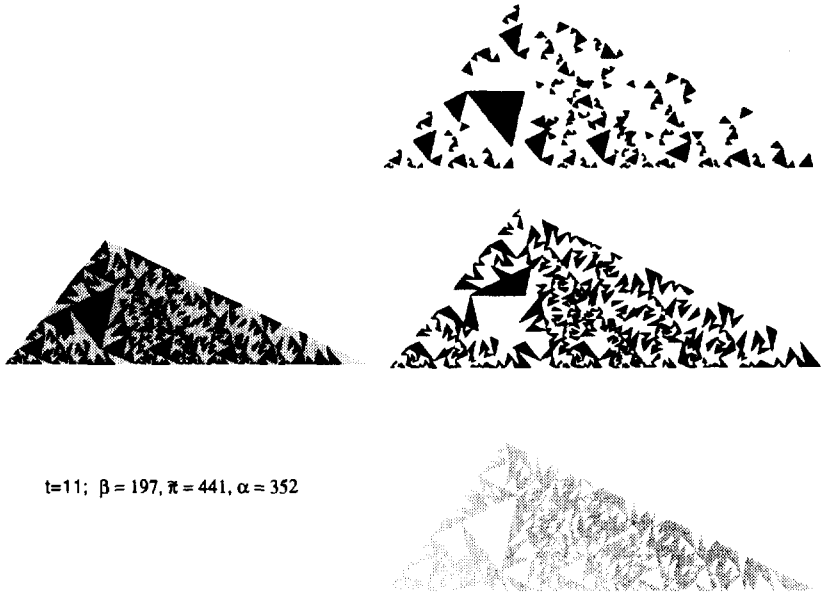

FIG. 16. Case of A_6. Partition of a triangle $\langle 4, 2, 1\rangle$ $\pi/7$ as a union of 197 + 441 + 352 triangles belonging to three congruent families. Step $t = 11$.

structure could be discussed in terms of our triangular dissections but we did not study this subject here.

5. Remarks about the Projection Technique

We have seen in the first part of this article how to generalize the dissection techniques known to generate Penrose aperiodic tilings of the plane [20] and indexed by the golden number. This generalization gives triangular dissections indexed by other algebraic integers belonging to the family $4\cos^2(\pi/(n+1))$. Specialists of quasicrystals with pentagonal symmetry know that there is another quite powerful technique to generate Penrose tilings: The so-called projection technique [15] (or dimensional reduction technique). This technique has already been generalized to other cases [10, 18, 16]. One can start with $\mathbb{R}^p$ ($p = 5$ in the case of Penrose tilings) decompose $\mathbb{R}^p$ into eigenspaces of the matrix ρ representing the generator of the group $\mathbb{Z}_p$. It is actually convenient to use a self adjoint matrix like $M = \rho + \rho^\dagger$, so that we obtain a decomposition of $\mathbb{R}^p$ into eigenspaces corresponding to real eigenvalues. One then chooses a real decomposition of $\mathbb{R}^p$ into eigenspaces $\mathbb{R}^p = D \times T \times W1 \times W2 \ldots$,

where D is associated with eigenvalue 2 and such that M acts on T by dilatation (eigenvalue > 1). From the definition of M (and the fact that $\rho^p = 1$), it is clear that spaces $T, W_1, W_2, \ldots$ are all two-dimensional. We choose the regular lattice $\mathbb{Z}^p$ (actually some finite part of it contained in a hypercube) and project $\mathbb{Z}^p$ on the space $T \times W1 \times W2 \times \cdots$ parallel to D. In this way we obtain a regular lattice related to the root lattice of A_{p-1}. We then choose several $2p$-gonal windows in the window spaces $W_1, W_2, \ldots$ and keep only those points that can be projected (parallel to the sum of the other eigenspaces) simultaneously within these windows (i.e., the points belonging to the common shadow of al the windows). The last step is to project the remaining points on the two-dimensional target space T. The necessity of choosing windows before projecting on T comes from the fact that the image would otherwise be dense. The obtained discrete point set has many "good" properties; in particular, it is crystal-like and characterized by an inflation multiplier τ. Many pictures of quasicrystals obtained by this technique have been published in the case of $\mathbb{Z}_5$. We have followed this technique in the case of $\mathbb{Z}_7$ and obtained Fig. 17. Here we set $M = -(g^2 + g^5)$, with $g^7 = 1$, approximate eigenvalues of M are $-2., 1.80194, 1.80194, -1.24698, -1.24698, 0.445042, 0.445042$, the two-

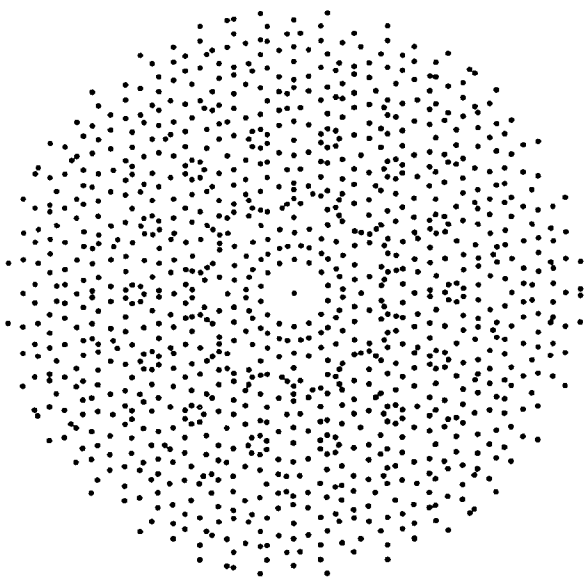

FIG. 17. A particular two-dimensional projection of the root lattice of A_6. The projector is obtained from the decomposition of R^7 into eigenspaces of $\rho + \rho^\dagger$ with $\rho^7 = 1$. The original points belong to the shadow of a four-dimensional window which is the product of two 14-gones.

dimensional target T is associated with $2\cos \pi/7 = 1.80194\ldots$ and the two other window spaces W_1 and W_2 with the two other eigenvalues. We start with $4^7 = 16{,}384$ lattice points in R^7, the intersection of the "shadows" in R^6 of two 14-gonal windows centered in W_1 and in W_2 contains 2119 points that are projected on T, i.e., in Fig. 17 (only lattice points have been drawn). We have also considered the choice $M = -(g^2 + g^3 + g^4 + g^5)$ and obtained very similar pictures. There is no direct correspondence between the number and locations of points (vertices of triangles) obtained after a dissection of t steps and the points obtained via the dimensional reduction technique. Indeed, the "order of arrival" of points obtained thanks to the projection technique is a function of the arbitrarily chosen size of windows and of the size of the chosen hypercube of $\mathbb{R}^5$. The dissection technique discussed previously looks more fundamental, in the sense that one can follow step by step the inductive algebraic process and the role of Jones algebras. It is, however, quite interesting to superimpose Fig. 17 (projection technique) with Fig. 18 (triangular dissection technique), both obtained in the study of the A_6 case.

The use of K-theory in the coding of aperiodic lattices has been advocated several times [2, 13]; such structures can be obtained, thanks to a projection technique, but the direct link with the inductive algebraic process—described by Brattelli diagrams—is then lost.

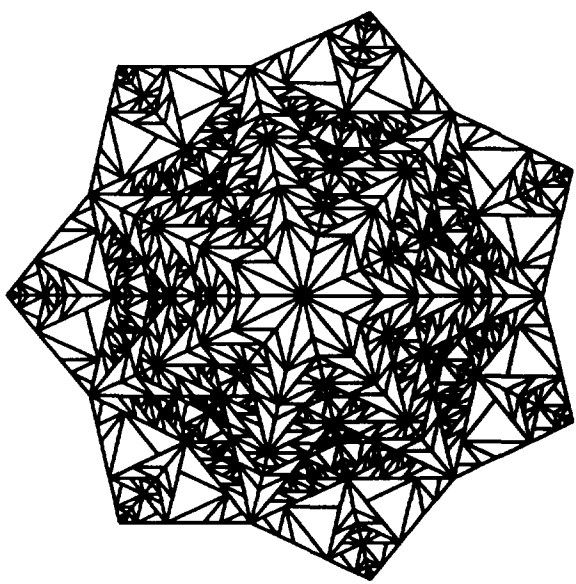

FIG. 18. Picture obtained after symmetry and seven-fold rotation of the A_6-fractal dissection of a triangle $\langle 4, 2, 1\rangle$ $\pi/7$.

The fractal aperiodic structures discussed in the present paper cannot be called "tilings" (since these triangular dissections usually involve triangles that are congruent but not isometric). The fact that they can be related to ADE Coxeter–Dynkin diagrams may come as a surprise and is maybe another of the many incarnations of Gabriel's theorem [11, 12].

The last figure (Fig. 18) is obtained by rotating a triangular dissection of order 7 and could, maybe, inspire children willing to play a fractal version of the game of hopscotch ("marelle").

ACKNOWLEDGMENTS

I thank the members of the Department of Mathematics of the University of Macquarie (Sydney) where this work started, in particular Professors J. Corbett and M. Adelman for their invitation. I also thank my colleagues from the Centre de Physique Theorique (in particular, G. Esposito Farese), in Marseille, for their interest and useful comments.

REFERENCES

1. O. BRATTELLI, *Trans. Amer. Math. Soc.* **171** (1972).
2. A. CONNES, "Introduction à la géometrie non commutative," Inter Editions, Paris, 1990. *Inst. Hautes Etudes Sci. Publ. Math.* **54** 1993.
3. A. CONNES, "Non Commutative Geometry," *Inst. Hautes Études Sci. Publ. Math.* **54** 1993.
4. A CONNES, "Seminaire Bourbaki, 37e année, 1984–85," No. 647.
5. M. GARDNER, "Penrose Tiles to Trapdoor Ciphers," Freeman, New York, 1989.
6. F. M. GOODMAN, P. DE LA HARPE, AND V. F. R. JONES, "Coxeter Graphs and Towers of Algebras," Math. Sci. Res. Inst. Publ. No. 14, Springer-Verlag, New York/Berlin, 1989.
7. B. GRÜNBAUM AND G. C. SHEPHARD, "Tilings and Patterns," Freeman, New York, 1987.
8. V. F. R. JONES, *Invent. Math.* **72** (1983), 1–25.
9. V. F. R. JONES, "Subfactors and Knots," CBMS, Regional Conference Series in Mathematics, No. 80, Amer. Math. Soc., Providence, Rhode Island, 1991.
10. A KATZ AND M. DUNEAU, *Phys. Rev. Lett.* **54** (1985), 2688–2691.
11. P. GABRIEL, Unzerlegbare Darstellungen I, *Manuscripta Math.* **6** (1972), 71–103.
12. I. N. BERSTEIN, I. M. GEL'FAND, AND V.A. PONOMAREV, *Russian Math. Surveys* **28** No. 2 (1973), 17–32; *Uspekhi Mat. Nauk* **28** No. 2 (1973).
13. J. KELLENDONK, Bonn-HE-92-26.
14. R. L. GRAHAM, D. E. KNUTH, AND O. TATASHNIK, "Concrete Mathematics," Addison–Wesley, Reading, Massachusetts, 1992.
15. P. KRAMMER AND R. NERI, *Acta Crystallogr. A* **40** (1984), 580–587.
16. W. F. LUNNON AND P. A. B. PLEASANTS, *J. Math. Pures Appl.* **66** (1987), 217–263.
17. A. OCNEANU, Quantized groups, string algebras and Galois theory for algebras in Operator algebra and applications, "London Math. Soc. Lecture Note Ser., Vol. 136 (Evans and Takesaki, Eds.), pp. 119–172, Cambridge Univ. Press, Cambridge, 1988.
18. P. A. B. PLEASANTS, in "Elementary and Analytic Theory of Numbers, Banach Center Publ. Vol. 17, pp. 439–461, PWN-Polish Sci., Warsaw, 1984.
19. N. TEMPERLEY AND E. LIEB, *Proc. Roy. Soc. London, Ser. A* **322** (1971), 251–280.
20. S. WAGON, "Mathematica in Action," Freeman, New York, 1992.